Наносистеми, наноматеріали, нанотехнології
Nanosistemi, Nanomateriali, Nanotehnologii
2025, т. 23, № 4, сс. 1217–1238
https://doi.org/10.15407/nnn.23.04.1217

PACS numbers: 61.72.Dd, 68.37.Hk, 68.43.Mn, 81.05.uj, 82.20.Pm, 82.60.Qr, 87.23.Cc

Investigation of the Kinetics and Thermodynamics of Chlorpheniramine Adsorption from Prepared Activated Nanocarbon

Rawa Mustafa Abdel Majeed[1], Noha Mohammad Yahya[1], and Raed H. AL-saqa[2]

[1]*College of Education for Girls, Department of Chemistry, University of Mosul, Mosul, Iraq*
[2]*Directorate General of Education in Nineveh, Ministry of Education, Mosul, Iraq*

This study produces a new type of activated nanocarbon using eucalyptus leaves from the forests around Mosul. The average particle size of this carbon produced is of 151.47 nm and is identified as nanocarbon. The drug chlorpheniramine is extracted from its aqueous solution. In this study, the Freundlich and Langmuir isotherms are used, where the Langmuir model fits the actual data for the analysed system better. This is evidenced by the results of high R^2 values of 0.9875 for Freundlich isotherm and 0.9935 for Langmuir one. Thermodynamic analysis of equilibrium adsorption shows that it is a spontaneous process with negative ΔG^0 values and results in a regular increase (negative ΔS^0 value) after the adsorption process. Physical adsorption forces ($\Delta H = -16.452$ kJ/mole) determine the bonding between the drug surface and the carbon one, and the adsorption process results in heat release. The three kinetic models are of pseudo-first order, pseudo-second order, and implicit molecular diffusion. The results show that the equilibrium adsorption follows the pseudo-second-order reaction equation, and the adsorption process is governed by multiple mechanisms in addition to molecular contact diffusion.

У цьому дослідженні одержано новий тип активованого нановуглецю з використанням листя евкаліпта з лісів навколо Мосула. Середній розмір частинок цього одержаного вуглецю становив 151,47 нм і був ідентифікований як нановуглець. Препарат хлорфенірамін був екстрагований з його водного розчину. У цьому дослідженні використано Фрейндліхову та Ленґмюрову ізотерми, де Ленґмюрів модель ліпше відповідає фактичним даним стосовно аналізованої системи. Це підтверджу-

ється результатами високих значень R^2: 0,9875 для Фрейндліхової ізотерми та 0,9935 для Ленґмюрової. Термодинамічна аналіза рівноважної адсорбції показала, що то був спонтанний процес з неґативними значеннями ΔG^0 і привів до реґулярного збільшення (неґативне значення ΔS_0) після процесу адсорбції. Фізичні сили адсорбції ($\Delta H = -16{,}452$ кДж/моль) визначали зв'язок між препаратом і поверхнею вуглецю, а процес адсорбції привів до виділення тепла. Три кінетичні моделі були: псевдопершого порядку, псевдодругого порядку та неявною молекулярною дифузією. За результатами, рівноважна адсорбція відповідає рівнянню реакції псевдодругого порядку, а процес адсорбції реґулюється кількома механізмами, окрім молекулярної контактної дифузії.

Key words: activated charcoal, eucalyptus trees, chlorpheniramine, nanocarbon, adsorption kinetic, adsorption thermodynamics.

Ключові слова: активоване вугілля, евкаліпти, хлорфенірамін, нановуглець, кінетика адсорбції, термодинаміка адсорбції.

(Received 3 September, 2024; in revised form, 24 September, 2024)

1. INTRODUCTION

One of the biggest problems in the modern world is environmental pollution, which has become more prevalent due to industrial development and population growth. Industry is considered one of the main sources of environmental pollution [1]. Because they contain hazardous chemical groups, chemicals or the products of their biological breakdown are among the contaminants that have an impact on the ecology of water [2]. In addition to its various household applications, it is essential for numerous economic effects, like agriculture, and it also has an impact on living things, like water. One of the challenges and issues of the modern era is the provision of drinkable water to cities and other sectors, river, lake, and groundwater water can. Due to their lack of water treatment units, hospitals are forced to discharge their heavy water into the main sewage network, where it eventually finds its way into rivers [3].

The difficulty with these pollutants stems from the fact that wastewater treatment plants are unable to remove them, reuse them, or otherwise benefit from them, which creates a number of issues that increase the amount of pollutants that end up in the river [4]. One kind of antihistamine medication that is released into rivers as a liquid contaminant is chlorpheniramine. One of the most pervasive pollution issues in the world, it has become imperative to find solutions and treat it. Governments have started to impose regulations and laws regarding the locations of laboratories and the treatment of water before it is released into the environment. As a

result, researchers in this field have developed low-cost adsorbent materials to combat pollution in all of its forms. Contaminated water and adsorbent material can be disposed of by reactivating the material, making it recyclable. In this way, adsorption is one of the most straightforward approaches to treating pollution.

The most well known isotherm models, which can be successfully applied to single-component systems, is the Freundlich equation. This model assumes that the adsorbents' surface is not homogeneous due to the irregularity of the potential energy on it because of the adsorption sites having varying levels of energy. The correlation coefficient (R^2) value can be used to express the strength of the linear relationship and determines the extent, to which the isotherm can accurately represent the experimental data for adsorption. The following equation can be used to express the linear model [5]:

$$\log q_e = \log K_F + n^{-1}\log C_e, \quad (1)$$

where K_F is Freundlich isotherm constant; q_e is amount of adsorbed material per gram of adsorbent, which is known as the adsorption capacity (at equilibrium) [mg/g]; C_e is concentration of the remaining material, which is the non-adsorbed at equilibrium [mg/L]. When drawing the relationship between $\log q_e$ *versus* $\log C_e$, it gives a straight line with a slope equal to $1/n$, which represents a measure of the intensity of adsorption, and a cross section equal to $\log K_F$, which is a function of the adsorption capacity, whereas the value of n indicates the best value for obtaining the adsorbent feature and the degree of non-openness to the adsorbent feature layer, where, when it is only limited between 1–10, this means that adsorption is good and preferred, but, when the value n is less than 1, this adsorption is preferred and not preferable, but, when $n = 1$, this adsorption is linear, whereas when $n < 1$, the adsorption is chemical, but, when $n > 1$, there is physical adsorption [6].

This model assumes that molecules adsorb on a specific number of openings (pores) located on a specific weight of the adsorbent surface, which are energetically equivalent, and each hole can hold only one adsorbed molecule; the molecules adsorbed on the adsorbent surface do not interfere with each other or with other attacking molecules present in the solutions. Therefore, a single layer of adsorbed molecules is formed on the adsorbent surface. According to this model, the adsorption phenomenon is rapid in the beginning and then reaches a state of equilibrium after the relative rate of speed equals due to the attachment of molecules on the surface of the adsorbent and the rate of their return to the solution [7]. According to this model, the amount of adsorbed material is proportional to the part exposed to the adsorption phenomenon, while the

amount of returning particles is proportional to the covered part of the surface. This model can be expressed by linear equation [8]:

$$\frac{C_e}{q_e} = \frac{1}{bQ_{\max}} + \frac{C_e}{Q_{\max}}; \tag{2}$$

here, b is Langmuir isotherm constant, $Q_{\max}$ is maximum theoretical capacity for adsorption of the adsorbent material; C_e and q_e are remaining concentration and adsorption capacity at equilibrium, respectively. To obtain accurate information that explains the mechanism of adsorption and the kinetic forces affecting it, kinetic models were studied on the studied drug as follow.

Lagergren proposed the first description of the kinetic data for adsorption through the pseudo-first-order equation, which is considered as the first equation used to describe the rate of adsorption based on its capacity, and after that, it was used by many researchers. Pseudo-first-order equation can be written [10] as

$$\ln\left(q_e - q_t\right) = \ln q_e - k_1 t. \tag{3}$$

In order to apply this model to practical data for adsorption, by plotting the relationship between $\ln(q_e - q_t)$ *versus* time t, it must give a linear relationship and a match must be obtained between the calculated and practical adsorption capacity values.

This model is also used to describe the kinetics of adsorption, as this model explains how the rate depends on the adsorption capacity of the solid adsorbent and not on the concentration of the adsorbent. Unlike the other kinetic models, it predicts the behaviour of adsorption along the time period of adsorption; this is consistent with an adsorption mechanism that includes a step that determines the rate, which may include countervailing forces through the sharing or exchange of electrons between the solution and the adsorbent, where the pseudo-second-order equation can be expressed [11]:

$$\frac{1}{q_t} t = \frac{1}{k_2}(q_e)^2 + \frac{1}{q_e} t. \tag{4}$$

In order for this model to apply to practical adsorption data, by plotting the relationship between t/q_t *versus* time t, it must give a linear relationship, and a match must be obtained between the calculated and practical adsorption capacity values [12]. It is also possible to use the adsorption rate constant k_2 to find the value of the initial pseudo-second-order adsorption speed (h) [11] as follows:

$$h = k_2(q_e)^2. \tag{5}$$

The overall rate of adsorption will be determined by the slowest step, which may be diffusion from the outer boundaries of the liquid to the adsorbent surface, or the implicit molecular diffusion within the pores of the adsorbent material. The rate of adsorption on the active sites is assumed to be fast, and one of the important things that must be found and determined is the potential rate of speed specific to the adsorption mechanism. According to Morris–Weber [13], if the implicit molecular diffusion is the controlling factor, depending on the reaction rate, the process of removing adsorbed materials changes with the square root of time. As a result, it is possible to calculate the rate of adsorption speed by calculating the adsorption capacity of the adsorbent as a function of the square root of time, as the implicit molecular diffusion model can be represented [14, 15] as follows:

$$q_t = K_{diff} t^{1/2} + C; \quad (6)$$

K_{diff} represents the rate constant for implicit molecular diffusion [mg·g^{-1}/min$^{1/2}$], while C is the value of the cross-section [mg/g]. The value of K_{diff} can be found from the slope of the straight line.

The aim of the study is to prepare the activated carbon from an available and cheap raw material, estimate the adsorption capacity, determine the optimal conditions, and study the adsorption kinetics and thermodynamics.

2. EXPERIMENTAL METHOD

2.1. Instruments

Different techniques and equipment were used to examine the samples, including UV-visible spectrophotometer (this two-track instrument is from Shimadzu Corporation of Japan (model 1800-UV)), sensitive electronic scale (model 200-CR sorted to four decimal places), drying oven (this oven is used for drying and carbonization), acidity meter (Jenway manufacturing, model 3510), water bath shaker (model Bs-11, Jwrio Tech, made in Korea), centrifuge (used to separate samples (separate precipitates from solutions); it originated from Germany, model Hermle Z200A, equipped by HERME LABORTECHNIK), SEM scanning device (model MIRA3LMU).

2.2. Chemical Materials

All chemicals, which were used, including hydrochloric acid, ethanol, potassium hydroxide, and distilled water (supplied by BDH-Fluka Company), synthesized activated carbon (SAC). A new type of

charcoal was prepared from eucalyptus leaves after cutting them, washing them several times, drying them under open air, and then placing them in an electric oven at a temperature of 105–110°C for 48 hours. The initial carbonization process was carried out by heating the leaves at a temperature of 350°C for three hours using a stainless steel bowl; then, the charcoal is cooled to room temperature, and for the purpose of performing the final carbonization, the charcoal powder was heated using a muffle furnace after mixing it with KOH in a ratio of 2.5:1 by weight of KOH:coal to a degree of 550°C for two hours. Then, the mixture was cooled and washed with distilled water several times until the pH of the washing water was equal to 7. Then, it was treated with a solution of 10% hydrochloric acid and heated for two hours. Then, it is cooled to laboratory temperature and washed until the acidity of the wash water reaches = 7.

Then, it was heated thermally using a solution of 0.1 N of KOH to transform it into charcoal with a basic character, and then, it was washed until the acidity of the washing water became = 9. Because the drug under study has an acidic character, then, the prepared activated charcoal was dried well, then, mechanically crushed, and molecular sieves were used to isolate it and preserved in sealed containers for subsequent study.

2.3. Adsorbent (Chlorpheniramine)

TABLE 1. The drug used and some of its properties.

Drug name	Structure	Colour	λ_{max}, nm
Chlorpheniramine	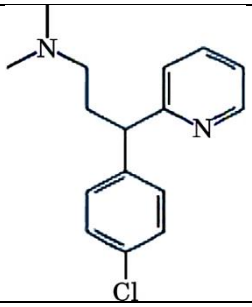	white	265

2.4. Determination of the Amount of Adsorbent

Both the adsorption efficiency and capacity are used to express the amount of the adsorbed substance by estimating the remaining amount of the substance in the solution. Since the drug that was studied is not coloured, the spectroscopic method in the UV region,

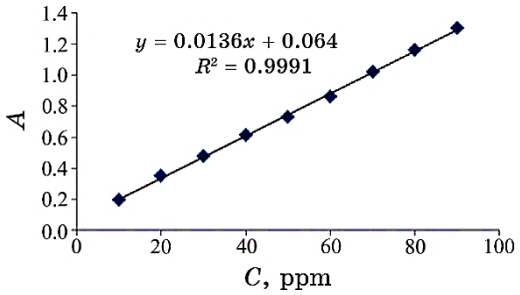

Fig. 1. Calibration curve for the drug theophylline.

which falls in the lower range of 300 nm, was used and calculated. The amount of adsorbed material is determined by the difference between the initial concentration and the remaining concentration in the solution. The calibration curve was adopted to find these concentrations. The adsorbed material, adsorption efficiency, and adsorption capacity were found through the following equations:

$$A = \varepsilon bCl, \tag{7}$$

$$q_e = \frac{C_i - C_e}{m} V_L, \tag{8}$$

where A represents the absorption, ε is the absorption coefficient, and C is the concentration; l represents the cell width ($l = 1$ cm); C_i represents the initial concentration, and C_e represents the remaining concentration, while $(C_e - C_i)$ represents the adsorbed concentration, which is symbolized by C_{ads}, while q_e represents the adsorption capacity; as for V_L, it is the volume of the drug solution in litres, and m is the weight of the adsorbed material [g]. All concentrations are in the unit [mg/L] ppm.

2.5. The Use of the Batch Method

All studies have been completed on the influence of factors on the adsorption process and its kinetic studies, which include applying the study in a one-shot method by changing some variables and fixing others, as follow.

Solutions of different concentrations of the drug were prepared in tightly sealed conical glass flasks under the same conditions. Then, quantities of adsorbent material from commercial activated carbon and prepared activated carbon were added to it, and it was shaken continuously at specific times and at a rate of shaking of 100 revolutions/minute using a water bath vibrator after adjusting

the temperature.

2.6. Determine the Maximum Wavelength and Calibration Curve

The greatest wavelength (λ_{max}) was determined at the highest absorption of the solution prepared from the drug under study by recording the absorption spectrum of the drug solution with an appropriate concentration, through which the highest wavelength of the drug solution was determined when the highest absorption value was read. Then, a solution of the drug at different concentrations was prepared, the absorption of the solution at those concentrations was measured, and then, the relationship between the intensity of absorption and the concentrations, to which the Beer–Lambert law must apply, was drawn. As found, the λ_{max} value of this drug is of 265 nm.

3. RESULTS AND DISCUSSION

3.1. Adsorbent Material

For the purpose of investigation, the surface shape of the synthesized activated carbon (SAC), a scanning electron microscopy (SEM) and x-ray diffraction (XRD) spectroscopy were used to examine the carbon model prepared in this study, as shown in Fig. 2.

Results of SEM measurements show a variation in the size of the particles of the prepared carbon (Fig. 2, *a*), and all of them were of nanosize: 43.69, 61.88, and 63.97 nm, as in Fig. 2, *b*. XRD was also used to study the crystalline shapes of the carbon surface, which gave the surface of the carbon prepared in this study has two bands at the location 2Theta, one of which is strong, located in the range

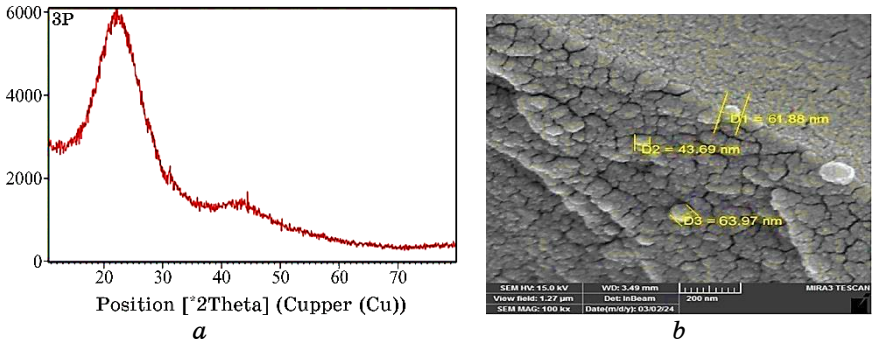

a *b*

Fig. 2. *a*—SEM, *b*—XRD shapes of the prepared carbon (SAC) surfaces.

TABLE 2. Effect of the adsorbent on the efficiency and capacity of adsorption at 60 minutes, a temperature of 25°C, a shaking speed of 100 rpm, and a volume of the drug solution of 25 ml.

Adsorbent	C_i, mg/L	Adsorbent material, mg	C_e, mg/L	Adsorption, %	q_e, mg/g
SAC	120 ppm	0.01	72.922	39.231	117.695
		0.02	61.723	48.564	72.846
		0.04	46.779	61.017	45.763
		0.06	32.854	72.621	36.310
		0.08	23.841	80.132	30.049
		0.1	16.371	86.357	25.907

20–30°, and the other is weaker, located in the range 42–48°. This gives an indication of the formation of nanosize particles.

3.2. The Effect of Adsorbent Weight

The results obtained, when studying the effect of the amount of adsorbent, are shown in Table 2.

From the above, the increasing the amount of adsorbent material increases the rate of adsorption directly, while the adsorption capacity, on the contrary, decreases due to the increase in the number of active sites on the surface of the adsorbent material to bind the molecules of the material to be adsorbed, and this result is consistent with previous results [16–18]. Therefore, we will limit our study in this research to the use of prepared coal because it is available in large quantities; in addition, it also gave results similar to commercial coal.

3.3. The Effect of Initial Concentration

Results obtained, when studying the effect of the initial concentration, are shown in Table 3. Results in Table 3 showed that the adsorption capacity increases with increasing concentration, while the adsorption efficiency (percentage of adsorption) decreases with increasing concentration. The reason for this may be due to the use of a fixed amount of adsorbent that contains a specific number of active sites. It leads to increased competition between drug molecules to bind to the active sites that leads to a larger amount of the drug remaining in the solution after the equilibrium process, which reduces the efficiency of adsorption, when calculated mathematically through the ratio between the amount of the adsorbed substance and the amount of the substance remaining in the solution.

TABLE 3. The effect of concentration on the efficiency and capacity of adsorption at 60 minutes, adsorbent is of 0.08 g, a temperature of 25°C, a shaking speed of 100 rpm, and a volume of the drug solution is of 25 ml.

Adsorbent	C_i, mg/L	C_e, mg/L	Adsorption, %	q_e, mg/g
SAC	70	1.321	98.112	17.169
	80	2.941	96.323	19.264
	90	6.189	93.123	20.952
	100	8.996	91.004	22.751
	110	12.412	88.716	24.397
	120	16.371	86.357	25.907
	140	25.071	82.092	28.732
	160	39.662	75.211	30.084
	180	60.982	66.121	29.754

TABLE 4. The effect of contact time on the efficiency and capacity of adsorption at a temperature of 25°C, an amount of charcoal prepared of 0.08 mg, an initial concentration of 40 ppm, a shaking speed of 100 rpm, and a volume of the drug solution of 25 ml.

Adsorbent	t_{im}, min	C_e, mg/L	Adsorption, %	q_t, mg/g
SAC	10	63.727	46.894	14.068
	20	48.812	59.323	17.797
	30	35.878	70.101	21.030
	40	24.823	79.314	23.794
	50	19.185	84.012	25.203
	60	16.371	86.357	25.907
	70	15.626	86.978	26.093
	80	15.626	86.978	26.093

3.4. Effect of Contact Time

Results obtained, when studying the effect of time, are shown in Table 4.

The time-effect results obtained in the above table show that the adsorption process is very fast in the first few minutes, and then, gradually slows down until the adsorption reaches equilibrium, because after reaching equilibrium, the adsorption process remains almost constant [19]. When the adsorption process reaches a point, where the rate of binding of adsorbent (drug) molecules to the surface of the adsorbent material is equal to the rate, at which other molecules are emitted from the adsorbent surface into the solution, this is called equilibrium state. It was found that the substance un-

der study reached the state of equilibrium in a time ranging between 70–80 minutes, and the occurrence of this difference in the speed of adsorption is due to the abundance of empty active sites present on the surface of the adsorbent material, which are qualified to bind to the adsorbent material at the beginning of the adsorption process. In addition to the fact that the concentration of the adsorbent material at the beginning of adsorption is high that facilitates the process of moving the molecules of the adsorbent to the surface of the adsorbent, and with the passage of time, the number of sites eligible for adsorption decreases and, with it, the competition between the molecules of the solution to bind to these sites increases, thus, resulting in a decrease in the speed of the adsorption process until the system reaches a state of equilibrium.

3.6. Effect of Temperature

The results obtained, when studying the effect of temperature, are shown in Table 5.

The results listed in the table above regarding the effect of temperature indicate that increasing temperature leads to a decrease in adsorption efficiency (percentage) and adsorption capacity, as increasing temperature leads to an increase in the process of the return of adsorbed molecules from the surface of the adsorbent to the solution (desorption) [20].

This is the result of the breaking of the bonding forces between the adsorbed material and the adsorbent surface, and this indicates that the adsorption process is exothermic [21] that indicates the physical nature of adsorption in the studied system, which applies exactly to Le Chatelier's principle [19]. This was proven in the thermodynamic study, which will be discussed in the later paragraphs.

TABLE 5. Effect of temperature on the efficiency and capacity of adsorption using the amount of adsorbent of 0.1 g, an initial concentration of 120 ppm, a time of 70 minutes, a shaking speed of 100 rpm, and a volume of the drug solution of 25 ml.

Adsorbent	Temperature, K	C_e, mg/L	Adsorption, %	q_e, mg/g	K_e
SAC	288	15.295	87.254	26.176	6.845
	298	15.626	86.978	26.093	6.679
	308	17.859	85.117	25.535	5.719
	318	22.936	80.886	24.266	4.231
	328	28.784	76.013	22.804	3.168
	338	32.390	73.008	21.902	2.704

3.7. pH Effect

The results obtained, when studying the effect of acid function, are shown in Table 6.

From the table above resulting from the effect of the acid function, we noticed that the capacity and efficiency of adsorption decrease clearly, when moving with the acid function from the acidic medium to the neutral and then basic. It was found that the adsorption process occurs in different acidic functions and is least in the basic medium [22].

3.8. Effect of Solvent

In Table 7, results obtained, when studying the effect of the sol-

TABLE 6. Effect of acid function on the efficiency and capacity of adsorption at a time of 70 minutes, an initial concentration of 40 ppm, a temperature of 25°C, an amount of adsorbent material of 0.08 g, a shaking speed of 100 rpm, and a volume of the drug solution is 25 ml.

Adsorbent	pH	C_e, mg/L	C_{ads}, mg/L	Adsorption, %	q_e, mg/g
SAC	2	9.572	110.428	92.023	27.607
	3	13.250	106.75	88.958	26.687
	4	14.959	105.041	87.534	26.260
	5.4	15.626	104.374	86.978	26.093
	7	19.870	100.130	83.441	25.032
	9	27.921	92.079	76.732	23.019

TABLE 7. Effect of the solvent using ethanol on the efficiency and capacity of adsorption, using the natural acid function at a time of 70 minutes, an initial concentration of 40 ppm, a temperature of 25°C, an amount of adsorbent material of 0.08 mg, a shaking speed of 100 rpm, and a volume of the drug solution of 25 ml.

Adsorbent	Water:ethanol, %	C_e, mg/L	C_{ads}, mg/L	Adsorption, %	q_e, mg/g
SAC	0:100	15.626	104.374	86.978	26.093
	10:90	21.343	98.657	82.213	24.664
	20:80	29.986	90.014	75.011	22.503
	30:70	41.875	78.125	65.104	19.531
	40:60	58.986	61.014	50.845	15.253
	50:50	73.174	46.826	39.021	11.706
	60:40	88.291	31.709	26.424	7.927
	70:30	107.877	12.123	10.102	3.030

vent, are shown. These results regarding the effect of the solvent indicate that the efficiency and capacity of adsorption decrease with an increase in the percentage of ethanol, which is a decrease in the percentage of water compared to an increase in the percentage of ethanol in the mixture, which is a decrease in the dielectric constant of the solvent, as it is known that water is the highest valuable solvent in its dielectric constant, which is of 80 that is higher than for ethanol, *i.e.*, 65. Therefore, mixing it with ethanol produces solvents with a lower dielectric constant [23]. Increasing the dielectric constant of the solvent leads to an increase in the tendency of the solute to move towards the surface of the adsorbent material more than its tendency towards molecular interactions of the solute–solute and solvent–solute types. Therefore, we find that the adsorption efficiency increases with the increase in the dielectric constant of the solvent.

3.9. Calculating Thermodynamic Parameters

Thermodynamic functions are among the important variables, which give a distinct interpretation, when studying the adsorption process. They explain the nature of the system studied, as well as the type of forces, which control it, and the course of the adsorption process. In addition, they can give an idea of the type of molecular interactions, which can occur during the adsorption process and have a major role in determining its competence. The heat of adsorption can be found from the Van't Hoff equation, which represents the relationship between temperature and the equilibrium constant:

$$K = K_0 \exp\left(-\Delta H/(RT)\right), \tag{10}$$

where ΔH represents the heat of adsorption, K represents the equilibrium constant for adsorption, while K_0 represents a constant value. Taking ln for both sides, we get the following form:

$$\ln K = \ln K_0 - \Delta H/(RT). \tag{11}$$

The value of ΔH can be found by drawing the relationship between ln$K$ *versus* the reciprocal temperature $(1/T)$, which gives a straight line with a slope equal to $-\Delta H/R$, and by knowing the value of the equilibrium constant for adsorption, which can be found from the ratio between concentrations of the adsorbed material remaining in the solution:

$$K = C_{ads}[\text{mg/L}]/C_e[\text{mg/L}]. \tag{12}$$

It is possible to find the value of ΔH and then find the other thermodynamic functions (ΔS^0, ΔG^0) through the following equations:

$$\Delta G^0 = -RT \ln K = -\Delta H - T\Delta S^0 , \quad (13)$$

$$\Delta S^0 = (\Delta H - \Delta G^0)/T . \quad (14)$$

The value of ΔG^0 represents the change in the standard free energy at any stage of adsorption, while ΔG represents the zero value and the free energy, when the equilibrium process is constant. Therefore, the value of ΔS^0 was found, which represents the state of the system at any stage of adsorption stages [24, 25].

As for the figure that represents the linear relationship resulting from plotting ln$K$ *versus* $1/T$ by applying the Van't Hoff equation (11), through the drawing shown in Fig. 3, we find that the practical data of the studied system at equilibrium are subject to the Van't Hoff equation, which is inferred through the values of the correlation coefficient (R^2) for the straight line, and when looking

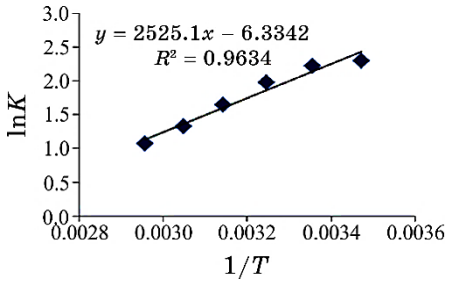

Fig. 3. Relationship between ln$K$ *versus* $1/T$ to calculate the thermodynamic functions for drug adsorption.

TABLE 8. Equilibrium constants and thermodynamic functions at equilibrium.

Adsorbent material type	Temperature, K	K_e	ΔG, kJ·mol^{-1}	ΔH, kJ·mol^{-1}	ΔS, J·mol^{-1}·K^{-1}
SAC	288	6.845	–4.605	–16.452	–41.135
	298	6.679	–4.704		–39.422
	308	5.719	–4.465		–38.918
	318	4.231	–3.813		–39.745
	328	3.168	–3.144		–40.573
	338	2.704	–2.795		–40.405

at the values of the thermodynamic functions as well as the values of the equilibrium constants, which were clarifying and listing them in Tables 8, as it is noted that they have changed as follow.

1. The values of the equilibrium constant K_e decrease with increasing temperature for the drug; this is consistent with what was found from studying the effect of temperature, namely, the efficiency of adsorption decreases with increasing temperature, that indicates that the forces responsible for the adsorption process are physical forces, as the increase in temperature leads to its breakdown. Then, the adsorbed molecules return to the solution, and this statement is firmly supported by the value of ΔH (-16.452 kJ·mol^{-1}).

2. Enthalpy change ΔH that was calculated is of a negative sign and indicates that the adsorption process is heat-emitting, while its values indicate that the forces responsible for the adsorption process are van der Waals forces, as the value obtained is less than 40 kJ·mol^{-1}) that is within the energy range of physical bonds [26].

3. The negative values of ΔS^0 give an indication of the state of order in the studied system that is worth noting is the strength of the interference and the preference for adsorption over desorption, and the fact that its values are within the certain range and are close at all temperatures. This supports that the system is of a physical nature, and that the role of entropy change is limited. In influencing the progress of the adsorption process, these results are supported by the values of the change in free energy ΔG^0, as its values indicate a decrease in the spontaneity of adsorption with the increase in temperature.

3.10. Adsorption Isotherms

3.10.1. Freundlich Isotherm

When applying Eq. (1) for this isotherm to the practical data for adsorption, by drawing the graphical relationship between logq_e *versus* logC_e, and through it, the values of the Freundlich constants (K_F, n) were calculated from the slope (n) and the cross-section (K_F) of the straight line, as shown in Fig. 4.

The results listed in Table 9 indicate that the Freundlich isotherm equation applies to the practical data of the well-studied adsorption system through the values of the correlation coefficient close to one. The values of n within the range between 1–10 also indicate that the adsorption system of the preferred type is governed by physical forces [27, 28], and this is consistent with what was shown by the values of ΔH, while the values of K_F are related to the adsorption capacity, and its high values indicate the efficiency of adsorption [29].

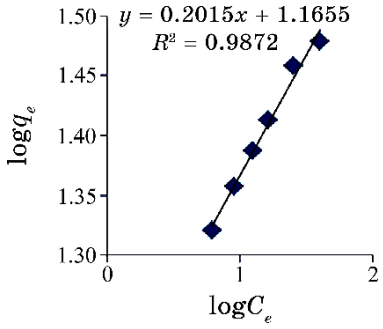

Fig. 4. Application of Freundlich isotherm to practical data for adsorption of the studied drug.

TABLE 9. Values of Freundlich constants (K_F, n) and correlation coefficient obtained by applying them to practical adsorption data.

N	K_F	R^2
4.962	14.639	0.9872

3.10.2. Langmuir Isotherm

When applying Eq. (2) to this model, by drawing the linear relationship between C_e/q_e *versus* C_e, it gives a slope equal to $1/Q_{max}$ and an intercept equal to $1/(bQ_{max})$ [34].

Figure 5 shows that excellent linear relationships were obtained through high correlation-coefficient values (0.9955), and thus, a conclusion can be reached that the practical results of adsorption for the systems under study showed greater agreement with this isotherm in describing the adsorption process than its application to the Freundlich isotherm.

The value of the Langmuir constant (b), which represents the bond strength between the molecules of the adsorbed substance on the adsorbent surface, is small. This means that the bond strength is weak and indicates that the adsorption is physical, and this supports the value of ΔH obtained from the thermodynamic study [30]. We also noticed that the value of the maximum theoretical adsorption capacity (Q_{max}) does not depend on the nature of the adsorbent material alone, but rather on other matters related to the nature of the adsorption system, including the nature of the adsorbed material and the aggregates associated with it, the surface area, the geometric shape, the method of its attachment to the adsorbed surface, as well as the interactions between the adsorbed molecules on the surface and the attacking ones to compete for the remaining sites and between them on the other hand [31].

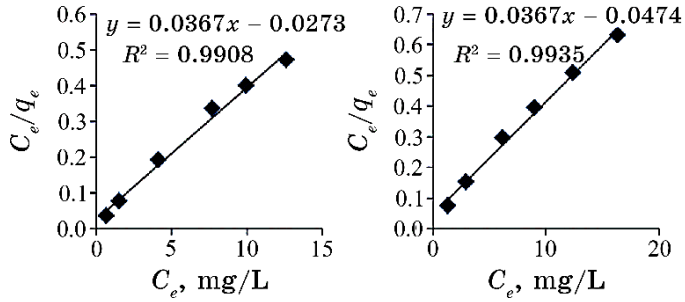

Fig. 5. Application of the Langmuir isotherm to experimental drug adsorption data.

TABLE 10. Values of the Langmuir constants (b, Q_{max}) and the correlation coefficient obtained by applying them to practical adsorption data.

Q_{max}, mg/g	b, L/mg	R^2
27.247	1.344	0.9935

3.10.3. Kinetic Study

3.10.3.1. Pseudo-First-Order Equation

The pseudo-first-order equation model, Eq. (3), was applied by drawing the relationship between $\ln(q_e - q_t)$ *versus* t with the time per minute to obtain a linear relationship with the magnitude of its slope $-k_1$ and its intercept $\ln q_e$, and through it, values q_e and k_1 can be found. The shape and results obtained are shown in Fig. 6 and listed in Table 11.

Comparing the practical or experimental adsorption capacity with their theoretical values shown in Table 12, it was noted that these values are not identical and not close to each other and the values of the correlation coefficient R^2 are not good, as this situation can be explained as follows. It is the possibility of a kinetic application of this model at a certain stage of the adsorption process, but Langmuir equation (3) cannot be applied to a large extent with practical values of adsorption because the theoretical basis assumed by this equation deviates from the practical values and the diffusion of drug molecules through the pores of activated charcoal, the initial concentration of the drug cannot be in a linear relationship with the rate of adsorption, despite the linear relationship given by the application of that equation.

These results represent the initial stage of the adsorption process, and not at all time periods of the adsorption process, the process is fast in its beginning. In general, it can be concluded that the

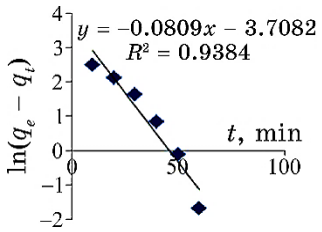

Fig. 6. Application of the pseudo-first-order model to experimental drug adsorption data.

TABLE 11. Practical and theoretical pseudo-first-order velocity constants, adsorption capacity, and the correlation coefficient.

$q_{e(exp)}$, mg/g	$q_{e(calc)}$, mg/g	k_1, min^{-1}	R^2
26.093	28.780	0.0809	0.9384

TABLE 12. Velocity constant, practical and theoretical pseudo-second-order adsorption capacity and correlation coefficient.

$q_{e(exp)}$, mg/g	$q_{e(calc)}$, mg/g	k_2, $g \cdot mg^{-1} \cdot min^{-1}$	h, $mg \cdot g^{-1} \cdot min^{-1}$	R^2
26.093	32.258	0.00211	1.436	0.9955

application of practical values for adsorption does not fully agree with the theoretical basis of the Lagergren equation for the adsorption system [31].

3.10.3.2. Pseudo-Second-Order Equation

Applying pseudo-second-order model to practical adsorption data by plotting the relationship between t/q_t *versus* time, it is also possible to use adsorption rate constant k_2 to find the initial pseudo-second-order adsorption speed (h) through Eq. (5).

The application of the pseudo-second-order model gave an excellent linear relationship, which indicates that a high correlation coefficient was obtained, as shown in Fig. 7, where the condition of this model matching the adsorption kinetics to the practical results of adsorption was achieved through the convergence of the practical values of the adsorption capacity at equilibrium $q_{e(exp)}$. With the values of $q_{e(calc)}$ calculated theoretically from the intersection of the straight line of the graph, for this reason, it can be said that the practical results of adsorption are subject to the false second-order model within the specified time period for the adsorption process [32]; one of the reasons, why the practical results of adsorption are

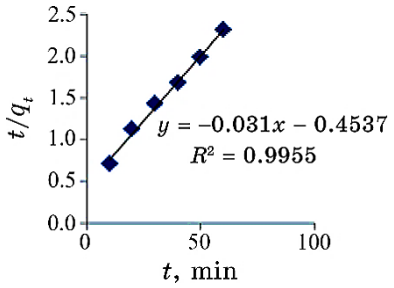

Fig. 7. Application of the pseudo-second-order model to experimental drug adsorption data.

subject to this model, may be the presence of influencing forces, which determine the speed of adsorption, such as the concentration of the adsorbent and the nature of the adsorption process, in addition to the path taken by the adsorbed solution molecules in the process of their transfer from the solution to the surface of the adsorbent and their spread through its internal pores.

As for the values of h, which is called as the initial rate of adsorption, the results calculated for it and shown in the table indicate that the higher the adsorption efficiency of the drug, the surface of the adsorbed material will occupied by the molecules of the adsorbed material faster that leads to a greater slowdown of the speed of the adsorption process. This is consistent with what was observed, when studying the effect of time on adsorption efficiency [33].

3.10.3.3. Intraparticle Diffusion Model

The implicit particle-diffusion model is applied to the practical data for adsorption by applying Eq. (6) and by drawing the relationship between the value of q_t *versus* the square root of time. The value of C gives evidence of the thickness of the outer layer of the solution boundaries and its effect, as a high value of C indicates this class has a greater influence [34].

The mechanics of the adsorption process can occur in three steps: firstly, the transfer of the adsorbed molecule from its location in the solution to the surface of the adsorbent after overcoming all the interfacial forces that hinder its movement in the solvent, then, its association with the active sites on the adsorbent surface, and finally, its spread through the internal pores of the adsorbent surface.

The mechanism of implicit molecular diffusion will be the only mechanism guiding the adsorption process, only when drawing the relationship between q_t *versus* $t^{1/2}$ gives a straight line passing

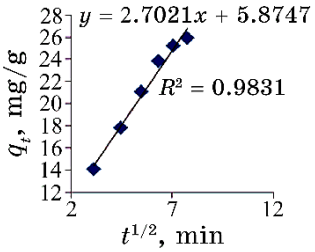

Fig. 8. Application of the implicit molecular-diffusion model to practical drug adsorption data.

TABLE 13. Values of the implicit molecular-diffusion constants and correlation coefficient.

C_i, mg/L	K_{diff}, mg·g^{-1}·min$^{-1/2}$	C, mg/g	R^2
120	2.7021	5.8747	0.9831

through the origin. Since this does not happen, this indicates that the process of implicit molecular diffusion plays an important role in the process of removing the drug from its aqueous solutions using activated charcoal.

However, the experimental results suggest that it is not the only mechanism controlling the drug adsorption, as shown in the results obtained in Table 13 and Fig. 8.

4. CONCLUSIONS

Dry fallen eucalyptus leaves cause environmental pollution and detract from the beauty and cleanliness of nature, but they have been transformed into a material that benefits the general economy of any country by producing activated nanocarbons from them.

Comparison of the two carbons shows that the synthetic nanocarbon used in this study is similar to commercial carbon and manifests high efficiency in removing pharmaceutical contaminants, especially, expired drugs, which are of the chlorpheniramine.

ACKNOWLEDGEMENTS

Authors would like to thank the University of Mosul, College of Education for Girls, thanks to Mr. Alaa Mohammed/New York Times/correspondent (for editing and reviser of the language), Mr. Faris M. Alhamadany (MSc Phys., University of Newcastle, U.K., 'work in Nineveh Medicine College').

REFERENCES

1. Jonathan Awewomom, Felicia Dzeble, Yaw Doudu Takyi, Winfred Bediakoh Ashie, Emil Nana Yaw Osei Ettey, Patricia Eyram Afua, Lyndon N. A. Sackey, Francis Opoku, and Osei Akoto, *Discover Environment*, **2**: Article No. 8 (2024); https://doi.org/10.1007/s44274-024-00033-5
2. Ewa Lipczynska-Kochany, *Areview. Chemosphere*, **202**: 420 (2018); https://doi.org/10.1016/j.chemosphere.2018.03.104
3. M. S. Holt, *Food and Chemical Toxicology*, **38**, Suppl. 1: S21 (2000); https://doi.org/10.1016/S0278-6915(99)00136-2
4. Ahmed Shabbir Khan, Ankur Anavkar, Ahmad Ali, Nimisha Patel, and Hina Alim, *Biosciences Biotechnology Research Asia*, **18**, Iss. 1: 9 (2021); http://dx.doi.org/10.13005/bbra/2893
5. A. Esmaeili, S. Ghasemi, and A. Rustaiyen, *American-Eurasian J. Agric. & Environ. Sci.*, **3**, Iss. 6: 810 (2008); https://doi.org/10.5897/AJB08.0
6. Alan L. Myers and Peter A. Monson, *Adsorption*, **20**: 591 (2014); https://doi.org/10.1007/s10450-014-9604-1
7. E. A. Al-hyali, T. Ra'ed, and N. H. Saleem, *Samarra Journal of Pure and Applied Science*, **3**, Iss. 4: 41 (2021); https://doi.org/10.54153/sjpas.2021.v3i4.292
8. Himanshu Gupta and Bina Gupta, *Desalination and Water Treatment*, **57**, Iss. 20: 9498 (2016); https://doi.org/10.1080/19443994.2015.1029007
9. Alírio E. Rodrigues and Carlos Manuel Silva, *Chemical Engineering Journal*, **306**: 1138 (2016); https://doi.org/10.1016/j.cej.2016.08.055
10. Yuh-Shan Ho and Augustine E. Ofomaja, *Journal of Hazardous Materials*, **129**, Iss. 1–3: 137 (2006); https://doi.org/10.1016/j.jhazmat.2005.08.020
11. S. Baup, D. Wolbert, and A. Laplanche, *Environmental Technology*, **23**, Iss. 10: 1107 (2002); https://doi.org/10.1080/09593332308618339
12. Yu Liu, *Colloids and Surfaces A: Physicochemical and Engineering Aspects*, **320**, Iss. 1–3: 275 (2008); https://doi.org/10.1016/j.colsurfa.2008.01.032
13. H. Esfandian, M. Parvini, B. Khoshandam, and A. Samadi-Maybodi, *Desalination and Water Treatment*, **57**, Iss. 37: 17206 (2016); https://doi.org/10.1080/19443994.2015.1086696
14. M. A. Rauf, S. B. Bukallah, F. A. Hamour, and A. S. Nasir, *Chemical Engineering Journal*, **137**, Iss. 2: 238 (2008); https://doi.org/10.1016/j.cej.2007.04.025
15. S. Mondal, S. Bhattacharyya, and P. Mitra, *Pramana*, **80**, Iss. 2: 315 (2013); https://doi.org/10.1007/s12043-012-0463-6
16. Abdullah M. Ali, Raed Alsaqa, and Nashwa Salhuddin Sultan, *International Journal of Thermodynamic*, **25**, Iss. 2: 33 (2022); https://doi.org/10.5541/ijot.1003950
17. Nouf F. Al-Harby, Ruwayda S. Almutairi, Noura Y. Elmehbad, and Nadia A. Mohamed, *Polymer Engineering & Science*, **63**, Iss. 8: 2336 (2023); https://doi.org/10.1002/pen.26380
18. Achraf Harrou, Elkhadir Gharibi, Hicham Nasri, and Meriam El Ouahabi, *SN Applied Sciences*, **2**, Iss. 2: 277 (2020); https://doi.org/10.1007/s42452-020-2067-y
19. P. S. Kumar, S. Ramalingam, C. Senthamarai, M. Niranjanaa, P. Vijayalakshmi, and S. Sivanesan, *Desalination*, **261**, Iss. 1–2: 52 (2010);

https://doi.org/10.1016/j.desal.2010.05.032
20. Momina, Shahadat Mohammad, and Suzylawati Isamil, *Journal of Water Process Engineering*, **34**: 101155 (2020); https://doi.org/10.1016/j.jwpe.2020.101155
21. Mo Fabio L. Leite, Carolina C. Bueno, Alessandra L. Da Ryz, Ervino C. Ziemath, and Osvaldo N. Oliveira Jr., *International Journal of Molecular Sciences*, **13**, Iss. 10: 12773 (2012); https://doi.org/10.3390/ijms131012773
22. H. A. Awala and M. M. El Jamal, *Journal of the University of Chemical Technology and Metallurgy*, **46**, Iss. 1: 45 (2011); https://journal.uctm.edu/node/j2011-1/6_Jamal.pdf
23. Peiming Wang and Andrzej Anderko, *Fluid Phase Equilibria*, **186**, Iss. 1–2: 103 (2001); https://doi.org/10.1016/S0378-3812(01)00507-6
24. Maryam Yazdani, Niyaz Mohammad Mahmoodi, Mokhtar Arami, and Hajir Bahrami, *Separation Science and Technology*, **47**, Iss. 11: 1660 (2012); https://doi.org/10.1080/01496395.2011.654169
25. Ibtihal A. Mawlood, Wahran M. Saod, Ahmed S. Al-Rawi, Abdulsalam M. Aljumialy, and Nahla Hilal, *Environmental Monitoring and Assessment*, **196**: Article No. 364 (2024); https://doi.org/10.1007/s10661-024-12525-1
26. M. A. Lala, T. E. Ntamu, O. A. Adesina, L. T. Popoola, A. S. Yusuff, and A. A. Adeyi, *Scientific African*, **20**: e01633 (2023); https://doi.org/10.1016/j.sciaf.2023.e01633
27. Asaad F. Hassan and Hassan Elhadidy, *Journal of Environmental Chemical Engineering*, **5**, Iss. 1: 955 (2017); https://doi.org/10.1016/j.jece.2017.01.003
28. Anchal Sharma, Nitin Kumar, Ackmez Mudhoo, and Vinod Kumar Garg, *Journal of Environmental Chemical Engineering*, **11**, Iss. 2: 109506 (2023); https://doi.org/10.1016/j.jece.2023.109506
29. Kheira Chinoune, Kahina Bentaleb, Zohra Bouberka, Abdelouahab Nadim, and Ulrich Maschke, *Applied Clay Science*, **123**: 64 (2016); https://doi.org/10.1016/j.clay.2016.01.006
30. Vojtěch Štejfa, Michal Fulem, Květoslav Růžička, and Ctirad Červinka, *The Journal of Chemical Thermodynamics*, **79**: 280 (2014); https://doi.org/10.1016/j.jct.2014.04.022
31. L. W Aarssen, *Journal of Vegetation Science*, **3**, Iss. 2: 165 (1992); https://doi.org/10.2307/3235677
32. Rohollah Ezzati, Saeid Ezzati, and Maryam Azizi, *Vacuum*, **220**: 112790 (2024); https://doi.org/10.1016/j.vacuum.2023.112790
33. Xia Wang, Qingjie Guo, and Tongtong Kong, *Chemical Engineering Journal*, **273**: 472 (2015); https://doi.org/10.1016/j.cej.2015.03.098
34. Stephanie A. Brocke, Alexandra Degen, Alexander D. MacKerell Jr., Bercem Dutagaci, and Michael Feig, *Journal of Chemical Information and Modeling*, **59**, Iss. 3: 1147 (2018); https://pubs.acs.org/doi/abs/10.1021/acs.jcim.8b00648